Spin-Enabled Plasmonic Metasurfaces for Manipulating Orbital Angular Momentum of Light

ARTICLE *in* NANO LETTERS · AUGUST 2013

Impact Factor: 13.59 · DOI: 10.1021/nl401734r · Source: PubMed

Guixin Li

University of Birmingham

Ming Kang

Tianjin Normal University

Shuang Zhang

University of Birmingham

Jensen Li

University of Birmingham

mac00 | ACSJCA | JCA10.0.1465/W Unicode | research.3f (R3.5.i3 HF03:4109 | 2.0 alpha 39) 2013/07/22 11:27:00 | PROD-JCAVA | rq_2681135 | 8/22/2013 10:54:04 | 4 | JCA-DEFAULT

NANO LETTERS

Letter

pubs.acs.org/NanoLett

Spin-Enabled Plasmonic Metasurfaces for Manipulating Orbital Angular Momentum of Light

Guixin Li,[†,⊥] Ming Kang,[‡,⊥] Shumei Chen,[†] Shuang Zhang,[∥] Edwin Yue-Bun Pun,[§] K. W. Cheah,[†] and Jensen Li*[,‡,∥]

[†]Department of Physics, Baptist University, Kownloon Tong, Kowloon, Hong Kong

[‡]Department of Physics and Materials Science and [§]Department of Electronic Engineering, City University of Hong Kong, Tat Chee Avenue, Kowloon, Hong Kong

[∥]School of Physics and Astronomy, University of Birmingham, Birmingham B15 2TT, United Kingdom

Supporting Information

ABSTRACT: Here, we investigate the spin-induced manipulation of orbitals using metasurfaces constructed from geometric phase elements. By carrying the spin effects to the orbital angular momentum, we show experimentally the transverse angular splitting between the two spins in the reciprocal space with metasurface, as a direct observation of the optical spin Hall effect, and an associated global orbital rotation through the effective orientations of the geometric phase elements. Such spin−orbit interaction from a metasurface with a definite topological charge can be geometrically interpreted using the recently developed high order Poincaré sphere picture. These investigations may give rise to an extra degree of freedom in manipulating optical vortex beams and orbitals using "spin-enabled" metasurfaces.

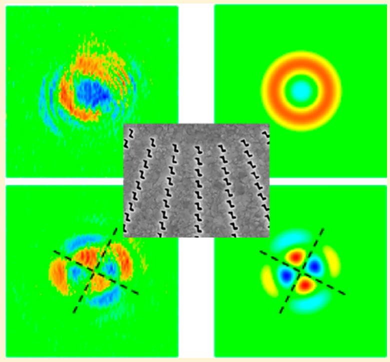

KEYWORDS: *Metasurface, spin−orbit interaction, optical spin Hall effect, orbital rotation*

Light can transport angular momentum through two different components, namely the orbital angular momentum (OAM) and the spin angular momentum (SAM).[1] During the transport of light, coupling between the orbital and the spin can occur. One of the important manifestations of this spin−orbit interaction is the celebrated spin-Hall effect for electron transport in semiconductors.[2,3] It is generalized to optics as the optical spin Hall effect (OSHE)[4−10] and had led to a group of interesting phenomena where the spin of light affects its orbital motion and vice versa.[11−14] The manipulation of this interaction can unlock the full potential of optical communication and information processing through an effective usage of both spins and orbitals.[15,16] On the other hand, metasurfaces, a class of structured interfaces with varying profiles of nanostructures, is currently under rapid development. Because of the usage of flexible artificial atoms, metasurfaces are able to introduce abrupt phase change to the transmitted or the reflected waves to alter either the linear or the orbital angular momentum of light.[17−21] In fact, in addition to pure wavefront engineering, metasurfaces are expected to provide a flexible and compact platform to control and generate spin−orbit interaction.[22] For example, a stronger version of OSHE with a polarization splitting of trajectory (in the linear transverse momentum) has been recently observed.[23] Here, we would like to investigate the spin−orbit interaction between SAM and OAM using metasurfaces constructed from geometric (Pancharatnam-Berry) phase elements.[11,12,20] Such a scheme has an advantage of being globally simple and therefore we can further exploit the flexibility of metamaterials in achieving different spin-induced effect on orbital manipulations. We show that such metasurfaces can induce polarization splitting in the angular direction by allowing the SAM to flow into the OAM. It can also induce different phase shifts among orbitals, yielding an overall effect of orbital rotation.[24,25]

In this work, we consider the effect of spin−orbit interaction when a metasurface with geometric phase elements interacts with the incident light. A typical metasurface of this type is showed in Figure 1. The design consists of concentric circular rings of the same kind of *Z*-shaped apertures etched on a gold surface. The rings have a periodicity of d = 300 nm, which is smaller than half of the incident wavelength (750 nm in the following experiments) so that the diffraction effect can be neglected. A SEM picture of the fabricated sample is showed in Figure 1c with caption for the detailed dimensions.

The spin−orbit interaction between the incident light and the metasurface comes from the geometric orientations of the metamaterial atoms. For a circularly polarized incident light, for example, right-handed circular polarization (labeled as $|-\rangle$ here), the transmitted light for the whole metasurface has a profile $|-\rangle t_{--} + e^{i2\alpha}|+\rangle t_{+-}$ where t_{ij} is the complex transmission

Received: May 12, 2013
Revised: August 6, 2013

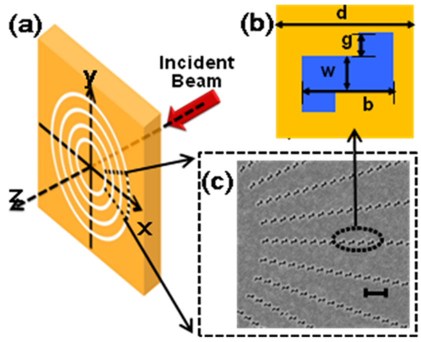

Figure 1. Metasurface constructed from *Z*-shaped apertures. (a) Schematic view of the metasurface. (b) A single unit cell of a *Z*-shaped apertures on gold, with b = 200 nm, w = 50 nm, and g = 65 nm. (c) Scanning electron micrograph of a fabricated sample (using focused ion beam), consisting of 60 rings of apertures with periodicity d = 300 nm in the radial direction. Scale bar is 600 nm (two periods along the radial direction).

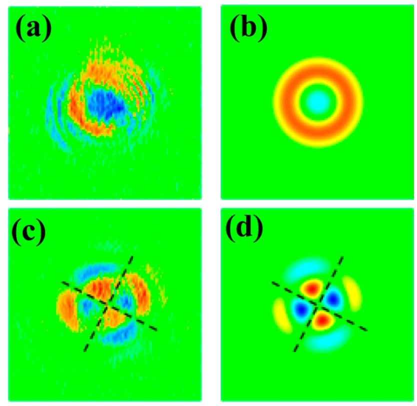

Figure 2. Optical spin Hall effect from the metasurface and the associated orbital rotation. (a) Experimental results and (b) theoretical predictions of the Stokes parameter S_3 for right-handed circular polarized incident light. (c,d) The corresponding results for incident light linearly polarized in the *y*-direction. More details on the beam profile measurement are given in Supporting Information.

coefficient (of the Jones matrix T) of a particular atom and α is the angular dependent orientation profile of the atoms. The spin−orbit interaction is provided by the varying atomic orientations in the angular (ϕ) direction for a metasurface of topological charge q ($q = \mathrm{d}\alpha/\mathrm{d}\phi$) where q = 1 in the case showed in Figure 1. The metasurface therefore flips the spin of the incident wave and induces an additional OAM ($\mp 2q$ for flipping $|\pm\rangle$) at the same time.[11,12] The quality of this spin−orbit interaction can be visualized by an intensity dip at the beam center in the cross-polarized light for the additional OAM (see Figure S-2 in Supporting Information). This effect happens in the phase and is exactly opposite for the two spins, in a way similar to another manifestation of OSHE with opposite phase shift (for the two spins) proportional to the transverse linear momentum.[23] Therefore, if we now shine both circular polarizations (e.g., a linear polarized light $|+\rangle + |-\rangle$) and assume the cross-polarization conversion being incomplete (nonzero t_{++} and t_{--}), the cross-polarized light ($\propto |t_{+-}|(e^{i2\alpha}|+\rangle + e^{i2\alpha}|-\rangle)$) interferes with the residual beam ($\propto |t_{++}|(|+\rangle + |-\rangle)$) and reveals the splitting between the two polarizations through an intensity profile either in the real space or in the reciprocal space (see Supporting Information for modeling details). This kind of polarization splitting is interpreted as an optical spin Hall effect (OSHE) in ref 7, which is originally based on exciton-polariton in a semiconductor cavity. It can be revealed by measuring the Stokes parameter $S_3 = I_L - I_R$. Figure 2a shows the measured Stokes parameter S_3 in the reciprocal space for the described metasurface with *Z*-shaped apertures for the right-handed circular polarized incident light. The two rings ($|+\rangle$ outside and $|-\rangle$ inside) are homogeneous in intensity in the angular direction without showing any angular splitting in this case as a control experiment. Now, we change the incident light to linear polarization along the *y*-direction, which is now a superposition of both circular polarizations. The corresponding measured S_3 is showed in Figure 2c. There is the mentioned splitting (showing up in red and blue colors) for the two circular polarizations in the angular direction for the same orbital as a direct observation of the OSHE. The splitting and also the number of lobes resemble to the Stokes parameter profile for the exciton-polariton case.[7] By using a metasurface, it allows us to have a more flexible control on the spin−orbit interaction (through the design of the metamaterial atoms) and the action can be performed within a very thin subwavelength thickness. Unlike the exciton-polariton case and also unlike the vertical splitting observed in the metasurface with V-shaped antennas,[23] the OSHE pattern for the current metasurface is not symmetric with respect to zero angle or zero vertical displacement in the reciprocal space. In fact, the pattern is rotated at an angle of around 27° in the clockwise direction (the dashed cross indicating the rotated nodal lines). For comparison, we numerically calculated t_{ij} using full-wave simulations (see Section 4 of the Supporting Information) and carried out the field integration in the transverse domain in order to obtain the far-field intensity profiles. They are plotted in Figure 2b,d with good agreement in the beam structure and also the rotation angle for the incident linear polarization.

To understand the action of the metasurface toward the incident beam, it is helpful to describe the action of a metasurface (of definite topological charge) using a high order Poincaré sphere picture.[26] Figure 3 summaries the actions after

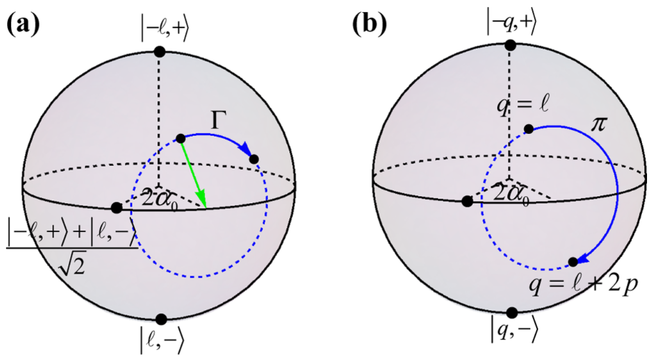

Figure 3. High-order Poincaré sphere for the action of a metasurface of topological charge $q = l + p$. (a) p = 0: Blue/green arrow shows the action of a metasurface constructed from identical wave plates of retardation phase shift Γ/linear polarizers with principal axis along direction of angle α_0. The actions correspond exactly to those in standard polarization control using homogeneous plates of zero topological charge. (b) $p \neq 0$: The head of arrow hops to the $(l + 2p)$-subspace while the tail of arrow stays in the original l-subspace, independent of using identical waveplates or polarizers to construct the metasurface. The conversion is complete for the case of a half-wave plate.

Jones matrix algebra with the t_{ij} coefficients. When we shine a beam with zero OAM ($l = 0$), Figure 3a (with substitution $l = 0$ and $q = 0$) corresponds to the Poincaré sphere for standard polarization control using a homogeneous plate of zero topological charge ($q = 0$). For example, a waveplate of phase retardation Γ and orientation at angle α_0 rotates the state around the direction $2\alpha_0$ on the equator of the Poincaré sphere by an angle Γ (the blue arrow in Figure 3a). A linear polarizer at an angle α_0 will project the state to the point of angle $2\alpha_0$ on the equator. If we now use a metasurface of topological charge $q = 1$ (as in Figure 2), the action of the metasurface is described by the Poincaré sphere showed in Figure 3b by putting $l = 0$ and $q = 1$. In this case, the Poincaré sphere mixes two sets of basis ($|0,+\rangle$,$|0,-\rangle$) and ($|-2,+\rangle$,$2,-\rangle$) (with first/second slot indicating OAM/spin in the Bra-ket notation). The metasurface rotates the state around the direction $2\alpha_0$ on the equator of the Poincaré sphere by an angle π (the blue arrow). Moreover, the action is independent of whether the metasurface is constructed from identical retardation wave plates or identical linear polarizers. The target state (head of arrow) hops to the subspace ($|-2,+\rangle$,$2,-\rangle$) (the same Poincaré sphere but with north/south pole as ($|-2,+\rangle$/$|2,-\rangle$) while there is a residual beam (tail of arrow) left behind in the subspace of zero OAM unless identical half-wave plates ($\Gamma = \pi$) are used to obtain complete conversion.

We note that the above geometric picture actually provides a natural framework to understand and to interpret the action of a metasurface of any topological charge q. The incident beam is decomposed into states individually spanned by $|-l,+\rangle$,$|l,-\rangle$[26] and the action can be investigated on each state written as

$$|\Psi\rangle = \cos\left(\frac{\Theta}{2}\right)|-l, +\rangle + \sin\left(\frac{\Theta}{2}\right)e^{i\Phi}|l, -\rangle \tag{1}$$

A metasurface of $q = l$ confines the action to the same high order Poincaré sphere (Figure 3a) while the action (T) for a metasurface of $q = l + p$ with a nonzero p is described by

$$T|\Psi\rangle - t_{++}|\Psi\rangle \propto \sin\frac{\Theta}{2}|-l - 2p, +\rangle + \cos\frac{\Theta}{2}e^{i(4\alpha_0 - \Phi)}|l + 2p, -\rangle \tag{2}$$

as the blue arrow in Figure 3b in mixing the l-subspace ($|\mp l$, $\pm\rangle$) and the $l + 2p$-subspace ($|\mp(l + 2p)$,$\pm\rangle$). All the described geometrical actions are simply promoted to these two subspaces. In eq 2, we have also assumed a single metamaterial atom can be "geometrically normalized" to have $t_{-+}/t_{+-} \approx \exp(i4\alpha_0)$ where α_0 is defined as the effective orientation of the atom for the ease of discussion. However, the application of the above approach for more general metamaterial atoms will be straightforward.

With such a geometric interpretation, the orbital rotation can be easily captured. The current metasurface with the Z-shaped apertures is designed to work like a metasurface constructed from identical wave plates whose retardation is around $\Gamma = 150°$ with an effective orientation $\alpha_0 = 27°$ by comparing the t_{ij} coefficients to those of a wave plate. Now, if we start with the same general state $|\psi\rangle$ and change the orientation of the waveplate from 0 (a control case without orbital rotation as we shall see in following experiment) to α_0, we have (from eqs 1 and 2)

$$\Delta\Theta = 0 \quad \text{and} \quad \Delta\Phi = 4\alpha_0 \tag{3}$$

which means a geometric rotation of angle $\Delta\Phi$ along the azimuth direction on the high-order Poincaré sphere of ($l + 2p$)-subspace. As a specific example for a state of spherical coordinate: ($\Theta = \pi/2\Phi$) on the equator, it has a profile $\hat{\mathbf{x}}\cos\gamma + \hat{\mathbf{y}}\sin\gamma$ where $\gamma = (l + 2p)\phi + \Phi/2$, the rotation on the high order Poincaré sphere in turns means that the orbital is physically rotated by an angle $-2\alpha_0/(l + 2p)$. Such a state, when interferes with the residual beam in the original l-subspace, creates the rotated OSHE pattern at an angle of -α_0 ($l = 0$, $p = q = 1$) in Figure 2.

As the orbital rotation is embedded in the geometric rotation on the high order Poincaré sphere, it can also be observed if we measure the orbital intensity profile through other polarizations as well. Figure 4c shows the far-field intensity profile for both x- and y-polarized transmitted light for an incident linear polarized light in the y-direction. For the cross-polarized light, the orbital rotation is observed with the same angle $-\alpha_0$, showed by the dashed cross. For the copolarized light, it is contaminated by the residual incident beam (the tail of blue arrow in Figure 3b) which is not rotated. However, the residual beam has a smaller amplitude (with conversion efficiency $\sin^2(\Gamma/2)$), the overall intensity profile thus still exhibits similar rotation behavior. For comparison, we have also fabricated a metasurface with rectangular apertures (the same Z-shaped apertures but without the two side arms) aligning in the radial direction with details given in Supporting Information. The rectangular apertures simply act like linear polarizers in this case. The cross-polarization and copolarization transmitted beam profiles are plotted in Figure 4a–d for both experimental and theoretical results as a control experiment without orbital rotation (dashed cross is at 0 and 90°). In essence, the effective orientations of the Z-shaped apertures (comparing to the rectangular ones) create an additional phase shift between the two spins. Through spin–orbit interaction, this phase shift is carried to the corresponding orbitals, inducing a global rotation to the overall intensity. Here, the observed orbital rotation induced by the materials can also be regarded as a mimic of an analogous geometric transformations for SAM and OAM.[24] Direct observation of the effect is possible also by exploiting the difference in t_{+-} and t_{-+} (similar to the current case) but with natural chiral medium, whose effect is too small to be detected.[25] Within the high order Poincaré sphere picture, the parallelism between the action of typical components like

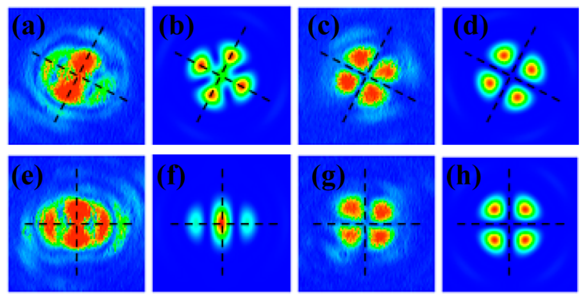

Figure 4. Orbital rotation observed from linear polarization. The first row shows the experimental measurement for the metasurface with Z-shaped apertures on (a) copolarization and (c) cross-polarization and the corresponding theoretical predictions (b) and (d) respectively. The second row shows the corresponding results for a metasurface with radially aligned rectangular apertures as control. Orbital rotation shows up in the cross-polarized and copolarized light as explained in text.

wave plates and polarizers on polarization control and the structured light control only occurs for metasurfaces of $q = l$ but not for metasurfaces of $q \neq l$. This is why we do not need optical active medium to rotate the beam state on the equator.

In conclusion, we have investigated the spin-induced effects on orbital angular momentum introduced by metasurfaces with geometric phase elements. We have found the spin-induced angular splitting between the two polarizations as a direct observation of OSHE. We can also control phase shifts between orbitals through the metamaterial atoms to induce a global orbital rotation by carrying the spin effects to orbitals. These can be described geometrically using a high order Poincaré sphere approach. The investigations are useful for understanding and for designing "spin-enabled" metasurfaces to manipulate optical vortex beams. It may also open up new functionalities in manipulating orbitals by transporting different effects in polarizations to orbitals through spin–orbit interaction.

■ ASSOCIATED CONTENT

Ⓢ Supporting Information

Figures S-1–S-3. This material is available free of charge via the Internet at http://pubs.acs.org.

■ AUTHOR INFORMATION

Corresponding Author

*E-mail: j.li@bham.ac.uk.

Author Contributions

$^{\perp}$G.L. and M.K. contributed equally to this work.

Notes

The authors declare no competing financial interest.

■ ACKNOWLEDGMENTS

This work is support by the Research Grants Council of Hong Kong (Project HKUST2/CRF/11G).

■ REFERENCES

(1) *Orbital Angular Momentum*; Allen, L., Barnett, S. M., Padgett, M. J., Eds.; IOP: Bristol, England, 2003.

(2) Murakami, S.; Nagaosa, N.; Zhang, S. C. Dissipationless Quantum Spin Current at Room Temperature. *Science* **2003**, *311*, 1348–1351.

(3) Sinova, J.; Culcer, D.; Niu, Q.; Sinitsyn, N. A.; Jungwirth, T.; MacDonald, A. H. Universal intrinsic spin Hall effect. *Phys. Rev. Lett.* **2004**, *92*, 126603.

(4) Onoda, M.; Murakami, S.; Nagaosa, N. Hall effect of light. *Phys. Rev. Lett.* **2004**, *93*, 083901.

(5) Kavokin, A.; Malpuech, G.; Glazov, M. Optical Spin Hall Effect. *Phys. Rev. Lett.* **2005**, *95*, 136601.

(6) Bliokh, K. Y.; Bliokh, Y. P. Conservation of angular momentum, transverse shift, and spin Hall effect in reflection and refraction of an electromagnetic wave packet. *Phys. Rev. Lett.* **2006**, *96*, 073903.

(7) Leyder, C.; Romanelli, M.; Karr, J. Ph.; Giacobino, E.; Liew, T. C. H.; Glazov, M. M.; Kavokin, A. V.; Malpuech, G.; Bramati, A. Observation of the optical spin Hall effect. *Nat. Phys.* **2007**, *3*, 628–631.

(8) Bliokh, K. Y.; Niv, A.; Kleiner, V.; Hasman, E. Geometrodynamics of spinning light. *Nat. Photonics* **2008**, *2*, 748–753.

(9) Hosten, O.; Kwiat, P. Observation of the spin Hall effect of light via weak measurement. *Science* **2008**, *319*, 787–790.

(10) Shitrit, N.; et al. *Nano Lett.* **2011**, *11*, 2038.

(11) Bomzon, Z.; Biener, G.; Kleiner, V.; Hasman, E. Space-variant Pancharatnam-Berry phase optical elements with computer-generated subwavelength gratings. *Opt. Lett.* **2002**, *27*, 1141–1143.

(12) Marrucci, L.; Manzo, C.; Parparo, D. *Phys. Rev. Lett.* **2006**, *96*, 163905.

(13) Zhao, Y. Q.; Edgar, J. S.; Jeffries; Gavin, D. M.; McGloin, D.; Chiu, D. T. Spin-to-orbital angular momentum conversion in a strongly focused optical beam. *Phys. Rev. Lett.* **2007**, *99*, 073901.

(14) Löffler, W.; Aiello, A.; Woerdman, J. P. Observation of orbital angular momentum sidebands due to optical reflection. *Phys. Rev. Lett.* **2012**, *109*, 113602.

(15) Molina-Terriza, G.; Torres, J. P.; Torner, L. *Phys. Rev. Lett.* **2001**, *88*, 013601.

(16) Wang, J.; et al. *Nat. Photonics* **2012**, *6*, 488.

(17) Yu, N.; Genevet, P.; Kats, M. A.; Aieta, F.; Tetienne, J. P.; Capasso, F.; Gaburro, Z. *Science* **2011**, *334*, 333.

(18) Sun, S.; He, Q.; Xiao, S.; Xu, Q.; Li, X.; Zhou, L. *Nat. Mater.* **2012**, *11*, 426.

(19) Ni, X.; Emani, N. K.; Kildishev, A. V.; Boltasseva, A.; Shalaev, V. M. *Science* **2012**, *335*, 427.

(20) Kang, M.; Feng, T.; Wang, H.-T.; Li, J. *Opt. Express* **2012**, *20*, 15882.

(21) Chen, X.; et al. *Nat. Commun.* **2012**, *3*, 1198.

(22) Litchinitser, N. M. *Science* **2012**, *337*, 1054.

(23) Yin, X. B.; Zilang, Ye,; Rho, J.; Wang, Y.; Zhang, X. Photonic spin hall effect at metasurfaces. *Science* **2013**, *339*, 1405.

(24) Allen, L.; Padgett, M. Equivalent geometric transformations for spin and orbital angular momentum of light. *J. Mod. Opt.* **2007**, *54*, 487.

(25) Loffler, W.; van Exter, M. P.; Hooft, G. W.; Nienhuis, G.; Broer, D. J.; Woerdman, J. P. Search for Hermite-Gauss mode rotation in cholesteric liquid crystals. *Opt. Exp.* **2011**, *19*, 12978.

(26) Milione, G.; Sztul, H. I.; Dolan, D. A.; Alfano, R. R. *Phys. Rev. Lett.* **2011**, *107*, 053601.